Theor Chem Acc (2010) 126:223–229
DOI 10.1007/s00214-009-0652-7

REGULAR ARTICLE

Structure and bonding of ethoxy species adsorbed on transition metal surfaces

Juan Radilla · Mercè Boronat · Avelino Corma · Francesc Illas

Received: 10 August 2009 / Accepted: 30 September 2009 / Published online: 15 October 2009

Abstract The interaction of the ethoxy radical with Cu(111), Ag(111), Pd(111) and Au(111) has been studied using a periodic density functional approach. The most stable adsorption site is the *fcc* with adsorption energies in the 1.1–2.2 eV interval. All analyses consistently indicate that ethoxy becomes negatively charged, that the presence of ethoxy slightly perturbs the electronic structure of the metallic surface, that the interaction is essentially of electrostatic character and not directional predicting a rather mobile species. The calculated adsorption energies are found to correlate almost linearly with the total net charge on the ethoxy moiety thus confirming that the electrostatic interactions dominate the bonding between this organic species and the underlying metallic surfaces.

Keywords Adsorbed ethoxy · Transition metal surfaces · Density functional theory (DFT)

Dedicated to the memory of Professor Jean-Pierre Daudey and published as part of the Daudey Memorial Issue.

J. Radilla · F. Illas (✉)
Departament de Química Física,
Institut de Química Teòrica i Computacional (IQTCUB),
Universitat de Barcelona, C/Martí i Franquès 1,
08028 Barcelona, Spain
e-mail: francesc.illas@ub.edu

J. Radilla
Departamento de Ciencias Básicas, Área de Química,
Universidad Autónoma Metropolitana-Azcapotzalco,
Av. San Pablo 180, CP. 02200 México, D.F., Mexico

M. Boronat · A. Corma
Instituto de Tecnología Química, UPV-CSIC,
Av. los Naranjos, s/n, Valencia, Spain

1 Introduction

Alkoxy radicals are ubiquitous in many chemical reactions taking place in completely different environments. For instance, these radicals play a central role in atmospheric chemistry since they are common intermediates in the oxidation of hydrocarbons [1, 2], are used in organometallic chemistry as ligands [3] or obtained as interesting products [4] in a number of selective reactions. Moreover, alkoxy species are present as intermediates in the selective oxidation of alcohols carried out either in solution [5] or through heterogeneous catalysts [6]. Precisely, the selective oxidation of alcohols to carbonylic compounds is one of the most important transformations in organic chemistry relevant to the production of fine and specialty chemicals [7–9] even if the use of inorganic environmentally unfriendly reactants is still widely used [6].

In order to replace current processes based on the use of toxic and expensive stoichiometric oxidizing reagents by green processes that use molecular oxygen as oxidant, it is necessary to develop active, selective and heterogeneous recyclable catalysts able to work at atmospheric pressure and low temperature. The new proposed catalysts involve a variety of transition particles (Cu, Ru, Pd, Ag, Au) conveniently supported [10–23] and different studies [10–23] agree that alkoxy species are common intermediates being located mainly not only at the surface of the transition metal particle but also on the oxide support [16, 18, 23]. Nevertheless, there is increasing evidence that naked metal particles in colloidal solutions [24] or supported on inert carbon [17] or silica [14, 20, 21] are highly active for selective alcohol oxidation. However, a detailed characterization of the atomic and electronic structure of alkoxy species is still missing and a detailed description of the bonding mode and characteristic vibrational features of the

alkoxy intermediate would be of interest to help the experimentalists to interpret their data, not always obtained in controlled ultra-high-vacuum conditions on single crystal surfaces. In particular, information about the vibrational features of adsorbed species is important since there is increasing evidence that adsorbed species can display a strongly distorted structure and, consequently, the corresponding infrared spectra of the adsorbed molecule can be very different from that of the gas phase species [25, 26]. Likewise, knowledge of the molecular properties of adsorbed alkoxy species can also provide a first step toward the understanding of the mechanism of the initial alcohol activation by these transition metal surfaces.

A number of detailed experimental studies exist aimed to characterize the structure and vibrational modes of adsorbed ethoxy species mainly not only on Cu(111) and Cu(100) surfaces [27–31] but also on bimetallic Ni/Pt(111) surfaces [32]. Likewise, a number of theoretical studies have investigated the geometry, stability and reactivity of methoxy on some transition metal surfaces such as Cu(111) [33–36], Ni(111) [37], Pd(111) [38] and Pt(111) [39] and of ethoxy on Cu(111) [36, 40] and Cu(100) [27] using either cluster or periodic surface models. These works focus mainly on the comparison between calculated and experimental data, especially to provide assignment to observed vibrational transitions, or on the reaction pathway for methanol or methoxy decomposition. However, a comparison of the main bonding features of these alkoxy radicals on different transition metal surfaces is still lacking. In this work, we report a detailed theoretical study of the geometry, stability and vibrational frequencies of ethoxy adsorbed on Cu(111), Ag(111), Au(111) and Pd(111) surfaces. This allows us to identify the active sites for adsorption, disclose trends on the bonding mechanism and also to extract important conclusions about the usefulness of vibrational frequencies to identify the type of transition metal surface.

2 Surface models and computational details

The Cu(111), Ag(111), Au(111) and Pd(111) transition metal surfaces have been represented through the repeated slab model with the slabs containing four metal layers and with a vacuum region of 12 Å between interleaved slabs. The slabs were constructed as usual from the bulk, using the lattice parameter which is consistent with the theoretical model used to compute total energies, and relaxing the two outermost atomic layers while keeping the bottom ones as in the bulk geometry. In order to avoid interaction between the adsorbates, a 2×2 supercell has been used (Fig. 1) which corresponds to a coverage situation of 0.25 ML.

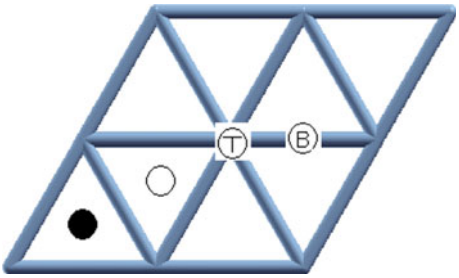

Fig. 1 The 2×2 surface supercell used in this work, adsorption sites explored are also indicated as follows: *solid* and *open circles* for *fcc* and *hcp* threefold sites, respectively. T and B circles for *top* and *bridge* sites

The interaction of the ethoxy (CH_3CH_2O) radical with the (111) metallic surfaces has been considered for the high symmetry sites displayed in Fig. 1. These are the usual on *top*, *bridge* and *fcc* and *hcp* threefold sites. In each case, the atomic coordinates of all ethoxy atoms as well as the two uppermost metallic layers have been fully optimized without any further constraint. In these calculations, the two lowermost layers have been kept fixed at the geometry optimized for the bulk metal, as in the case of the naked surfaces. In order to calculate the adsorption energy, the isolated ethoxy has also been fully relaxed in a box of the same size as that used in the surface calculations.

Total energies have been obtained from periodic density functional calculations using the Perdew–Wang (PW91) form of the Generalized Gradient Approach (GGA) for the exchange-correlation potential [41–43] as implemented in the VASP code [44, 45]. A plane wave basis set with a kinetic energy cutoff of 415 eV has been used to represent the valence density, with the effect of the core electrons in the valence density being taken into account by means of the Projected Augmented Wave (PAW) formalism [46] as implemented by Kresse and Joubert [47]. A suitable $5 \times 5 \times 1$ Monkhorst–Pack grid has been used to select the special *k*-points necessary to carry out numerical integrations in the reciprocal space [48]. Adsorption energies have been calculated as usual

$$E_{\mathrm{Ads}} = E_{\mathrm{M(111)-ethoxy}} - [E_{\mathrm{ethoxy}} + E_{\mathrm{M(111)}}]$$

with M = Au, Ag, Cu, Pd and $E_{\mathrm{M(111)}}$ representing the surface total energy, E_{ethoxy} the total energy of gas phase ethoxy and $E_{\mathrm{M(111)\text{-}ethoxy}}$ the total energy of the adsorption system. All calculations have been carried out without taking spin polarization into account except for the isolated radical in gas phase. For the adsorbed species, neglecting spin polarization does not introduce any significant difference because the unpaired electron of ethoxy fully delocalizes into the metal conduction bands.

The resulting structures have been characterized as minima by a pertinent frequency analysis. Vibrational

frequencies have been calculated by diagonalizing the block Hessian matrix corresponding to displacements of the coordinates of all the atoms of the ethoxy species. Visualization of structures and vibrational modes has been made with XcrySDen [49] and MOLDEN [50] codes, respectively. The electronic structure of the adsorption systems was analyzed through density of states (DOS) plots and Bader charge density analysis [51] with the implementation of Henkelman et al. [52] which allows to analyze the density issued from the VASP code. The charge density analysis was made from the self-consistent charge densities of the energy converged systems; total DOS plots were obtained from single point self-consistent calculations and from projected DOS refined with a denser $11 \times 11 \times 1$ Monkhorst–Pack grid to avoid numerical noise.

3 Results and discussion

3.1 Adsorption energies and adsorption geometries

The geometry optimization of the structure of adsorbed ethoxy starting from each of the high symmetry sites described in Fig. 1 converges to a stable situation where the oxygen atom of the ethoxy moiety points toward either the *fcc* or *hcp* high symmetry site, in agreement with results reported by Li et al. [40] for the case of the Cu(111) surface. For comparative purposes, calculations have also been carried out where the ethoxy oxygen atom is fixed above *top* and *bridge* sites allowing only vertical relaxation. Since in these two cases the optimization procedure has been carried out with symmetry restriction, it is clear that the structures thus found do not correspond to minimum energy stationary points in the corresponding potential energy surface. Obviously, the structures corresponding to adsorption above the *fcc* and *hcp* sites are always the most stable ones with the former being slightly preferred. For the Cu(111) surface, the calculated adsorption energies are very similar to those reported by Li et al. using a similar approach. The small differences (0.31 eV for adsorption at the *fcc* site) can be attributed to the different treatment of the interaction between valence and core electrons (PAW vs. ultrasoft pseudopotentials as used in Ref. [40]), to the use of a different supercell (2×2 vs. 3×3 as used in Ref. [40]) and to the fact that the present results account for the relaxation of the two uppermost metallic layers. The contribution of the surface relaxation to the adsorption energy was already estimated by Li et al. as of $\sim$0.1 eV, the rest is clearly due to the different treatment of the core–valence interaction. The situation with the O atom fixed above the *top* sites is the least stable and those where the O atom is fixed above *bridge* are intermediate although with some exceptions as one can see from the summary of results in Table 1. In fact, ethoxy adsorption on *bridge* sites is 0.20 eV less stable than on *hcp* sites for Cu(111) and Ag(111) but slightly preferred on Au(111) and Pd(111) indicating that in these two cases adsorption at the *hcp* site does not correspond to a local minimum. In any case, adsorption above the *fcc* site is always preferred and for this situation a clear trend in adsorption energy emerges with Cu > Ag > Pd > Au. In the forthcoming discussion, we will focus mainly on the *fcc* site and will also attempt to unravel the origin of the trend above commented.

Table 1 Adsorption energies (in eV) of ethoxy adsorbed on different positions above the transition metal surfaces studied in the present work

	top	*bridge*	*hcp*	*fcc*
Cu(111)	−1.50	−1.93	−2.12	−2.16
Ag(111)	−1.15	−1.60	−1.78	−1.81
Pd(111)	−1.31	−1.48	−1.38	−1.51
Au(111)	−0.84	−1.10	−1.08	−1.13

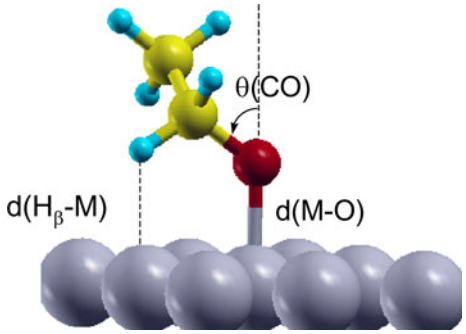

Fig. 2 Schematic view of ethoxy adsorbed on a (111) transition metal surface and definition of the relevant geometrical parameters (see text)

The optimized geometry of ethoxy adsorbed on Au(111) with a schematic description of the most relevant geometrical parameters analyzed in this work is depicted in Fig. 2 where d(O–M) is the shortest distance between the O atom of ethoxy and one metal surface atom, $d(H_\beta\text{–M})$ is the shortest distance from one hydrogen atom in beta position with respect to the O atom to one atom of the metal surface and θ(CO) is the tilting angle between the surface normal and the C–O bond axis. The optimized values of these parameters obtained for the most stable configuration with ethoxy adsorbed above the *fcc* site are summarized in Table 2 for Cu(111), Ag(111), Pd(111) and Au(111). Here, we find a more significant difference with the results reported by Li et al. [40] in the sense that the tilting θ(CO) angle calculated for ethoxy on Cu(111) is noticeable smaller than the one reported in [40]. The analysis of the chemical bond in a forthcoming subsection will provide a

Table 2 Relevant geometrical parameters, as defined in Fig. 2, for ethoxy adsorption above the most stable (*fcc*) site of the Cu(111), Ag(111), Pd(111) and Au(111) surfaces

	d(O–M)	d(H_β–M)	θ(CO)
Cu(111)	2.06	3.21	3
Ag(111)	2.33	3.16	3
Pd(111)	2.18	3.10	5
Au(111)	2.30	2.56	30

Distances are in Å and angles in degrees

Table 3 Most relevant calculated frequencies (in cm^{-1}) for ethoxy in the gas phase and adsorbed at the *fcc* site of Cu(111), Ag(111), Pd(111) and Au(111)

	Gas	Cu(111)	Ag(111)	Pd(111)	Au(111)
ν(CO)	1,067	1,116	1,113	1,106	1,107
ν(CC)	847	869	867	858	859
δ(OCC)	396	455	449	470	459

clear explanation for this difference. The interaction of the ethoxy radical with the metal surfaces causes a lengthening of the C–O bond length from 1.35 Å in the gas phase to 1.41–1.43 Å, while the C–C bond length remains unaltered and the OCC angle slightly closes from 118° to 110°–113°. The O–M distance varies from one metal to another in the order Cu < Pd < Ag ∼ Au, following the atomic radii trend. Interestingly, for the rest of configurations where the ethoxy oxygen atom is constrained to sit above the remaining high symmetry sites, the calculated values of these geometrical parameters are almost the same indicating that the interaction with the surface is not really directional and, hence, not dominated by covalent effects; we will come to this point later on.

3.2 Vibrational analysis

The calculated characteristic vibrational modes of ethoxy radical in the gas phase and adsorbed at the *fcc* site of the different transition metal surfaces studied in the present work are summarized in Table 3. These modes are the ones with components perpendicular to the surface and according to the metal surface selection rule likely to be observed in infrared experiments. Ethoxy adsorption on the metal surfaces considered causes a shift of ∼40–50 cm^{-1} to higher values in the ν(CO) stretching mode that is consistent with the increase in the CO bond length upon adsorption as discussed above. On the other hand, the variation in the calculated ν(CC) frequencies is considerably smaller as expected from the small change in the CC bond induced by adsorption. The OCC angles slightly close upon adsorption, and this is reflected in calculated frequencies for the δ(OCC) modes that are 50–75 cm^{-1} higher than in the gas phase.

Results in Table 3 also indicate that the shifts described above are insensitive to the metal substrate. This is a quite interesting feature because it indicates that these vibrational features can be used to identify the presence of ethoxy, for instance, in ethanol selective oxidation to acetaldehyde, but do not permit to infer the metallic substrate where this species is adsorbed. This insensitivity of the calculated vibrational frequencies is consistent with the insensitivity of the molecular structure of the adsorbed species toward underlying metallic substrate and, again, indicates that the interaction is not directional and, hence, not dominated by covalent effects.

3.3 Electronic structure analysis

We start the analysis of the interaction of the ethoxy radical on the different transition metal surfaces studied in the present work by inspecting the electronic structure through appropriate plots of the total DOS. In order to better visualize the effect of the adsorbate on the metallic surface electronic structure, we plot in Fig. 3 the total DOS of the naked surface together with the DOS corresponding to the adsorption system. Inspection of Fig. 3 reveals that the presence of the adsorbate does only produce a modest perturbation in the electronic structure of these metal surfaces. For all metals, the two plots are very similar with no new features clearly apparent in the DOS of the adsorption system compared to that of the naked surface. This, in principle frustrating picture, contains, however, the information about chemical bonding of ethoxy to metal surfaces. The absence of new features such as bonding and antibonding peaks strongly suggests that the covalent contributions are not dominant. This is in agreement with the information arising from the atomic structure and vibrational frequencies which are not sensitive to the type of metal surface. The absence of strong covalent interactions will lead to non-directional interactions and will also explain the rather flat potential energy surface landscape where the interaction of the adsorbate above different high symmetry sites does not lead to strong changes in the adsorption energy, except for the *top* site and this will become clear in forthcoming discussion.

To further corroborate the picture of the chemical bond arising from the total DOS, we plot in Fig. 4 the DOS of the two systems—naked surface and adsorption system projected in the d states of the metal atoms in the first atomic layer. This is because one expects the atoms of the first atomic layer to be precisely the ones interacting stronger with the adsorbate levels. The analysis of the projected DOS in Fig. 4 is fully consistent with the interpretation given above. The presence of the adsorbate has a

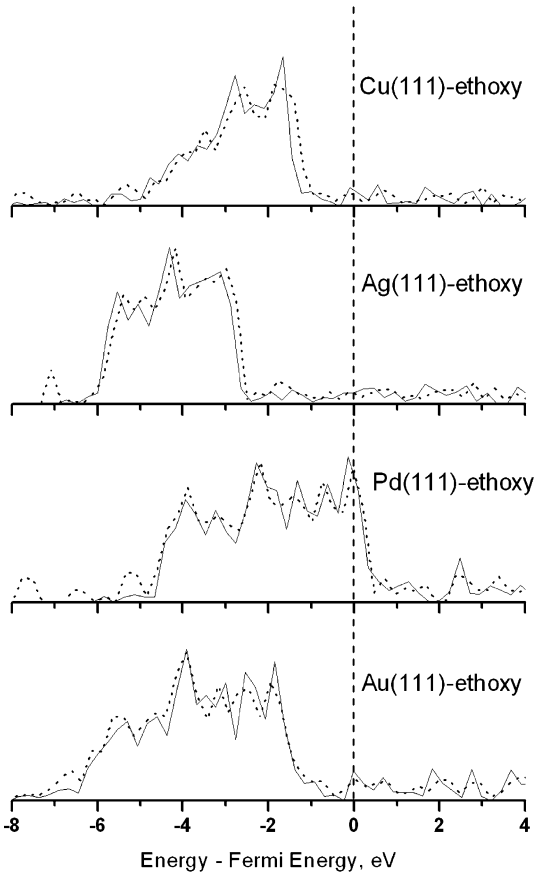

Fig. 3 Total density of states for the clean surface model (*solid line*) and for the surface with adsorbed ethoxy (*dotted line*)

minor effect on the d states arising from the atoms of the topmost layer and confirms that covalent effects are not responsible for the bonding interaction of this organic species on the metal surfaces. Still, the adsorption energies in Table 1 are sufficiently different for the different transition metal surfaces and require appropriate explanation. The conclusion that covalent contributions are not dominant together with the analysis of the atomic structure and vibrational frequencies, which points toward an interaction without specific directionality, strongly suggests that the chemical bond is dominated by the electrostatic interactions.

The analysis of electrostatic interactions between a metallic surface and an adsorbate is not a simple task. Ideally, one would like to perform an analysis following the constrained space orbital variation method which allows to decompose the interaction energy in various contributions [53, 54] but, unfortunately, this is not possible within a plane wave basis set and it has only recently been implemented for periodic calculations using Gaussian basis sets [55]. An alternative consists in exploring the net charges on the adsorbate following, for instance, the Bader method which relies in the use of topological atomic volumes rigorously defined [51]. Hence, the net charge on each atom of the ethoxy moiety has been obtained for each adsorption system following this procedure and the charge on the adsorbate obtained from the sum of atomic charge. The resulting charge for adsorbed ethoxy is −0.60, −0.58, −0.47 and −0.44 (a.u.) for Cu(111), Ag(111), Pd(111) and Au(111), respectively. The rather large negative charge indicates the tendency to acquire a closed shell configuration. The larger values correspond to Cu(111) and Ag(111) which are the surfaces with smaller calculated work function (4.98 and 4.54 eV for Cu(111) and Ag(111), respectively [56]) and the smaller values are those for the interaction with Pd(111) and Au(111) which are also the surfaces with larger calculated work function (5.38 and 5.22 eV, respectively [56]). However, apart from this qualitative trend, there is no direct relationship between the calculated adsorption energies and the surface work function values. A more quantitative trend emerges when the adsorption energies are plotted versus the net Bader charge on the adsorbate reported above. In fact, almost linear trend ($E_{ads} = 0.72 + 5.40Q_{Bader}$ with $R = 0.96$) in Fig. 5 fully confirms the conclusions reached from analysis of the atomic structure and of the DOS plots. The correlation in Fig. 5 is not perfect but explains the variation of the adsorption energy with the type metal surface, confirms that the interaction is essentially dominated by electrostatic interactions and, hence, without specific directionality, explains the relatively flat potential energy surface around the most stable position and also that the fact that interaction above the *top* site is the less favoured. This is simply because, without strong overlapping densities, the interaction above the *top* site corresponds to the largest contribution of the Pauli repulsion between the electron density of the metallic surface and the almost closed shell structure of the adsorbed molecule.

4 Conclusions

The adsorption of the ethoxy radical on Cu(111), Ag(111), Pd(111) and Au(111) has been studied by periodic density functional theory calculations on suitable slab models. The calculations reveal that while the most stable situation corresponds to the interaction of the molecule at the threefold *fcc* site with the adsorption energy ranging from 2.16 to 1.13 eV, the largest corresponds to Cu(111) and the smallest to Au(111). Calculations carried out for the molecule being forced to stay above other high symmetry sites indicate that the potential energy surface is very flat and, consequently, the adsorbed species is predicted to be rather mobile which may have consequences in the surface reactions involving this species.

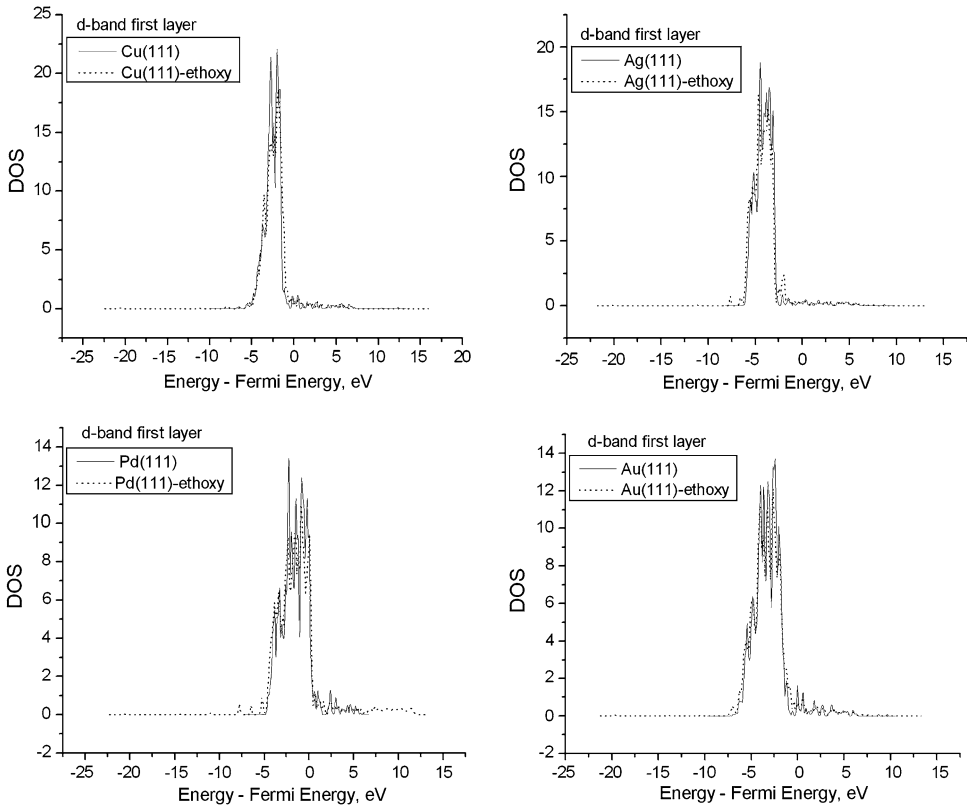

Fig. 4 Projected density of states for the clean surface model (*solid line*) and for the surface with adsorbed ethoxy (*dotted line*). The projection is carried out on the d states of the metal atoms in the topmost layer

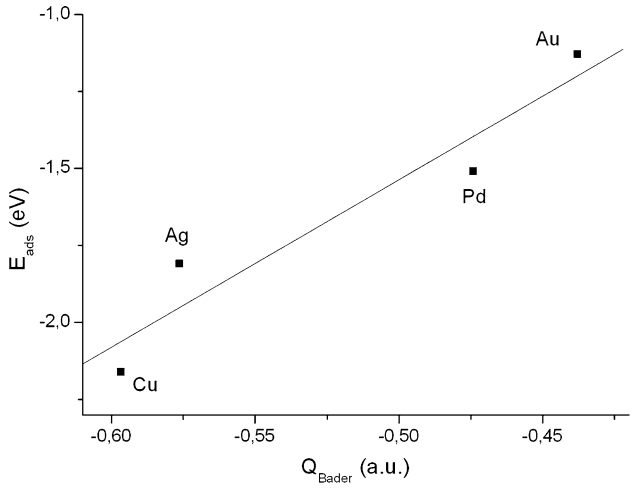

Fig. 5 Calculated adsorption energies as a function of the total Bader charge on the adsorbed ethoxy species

The structure of the adsorbed ethoxy radical is only slightly changed with respect to the gas phase values. More importantly, the effect of the type of metal surface on the geometry of the adsorbed molecules is quite small. This is also the case for the vibrational frequencies of the adsorbed species and, in particular, for the modes that can be experimentally observed. This result implies that while vibrational spectroscopy can be used to identify the presence of ethoxy on a given surface, for instance of a catalyst, the information from the recorded spectrum will not provide information about the active site. The insensitivity of the adsorbed molecule geometry and vibrational features with respect to the type of metal surface indicates that the interaction is not directional and not dominated by covalent effects. This is confirmed by analysis of the DOS plots which shows that the presence of the adsorbate does only introduce a small perturbation in the electronic structure of the underlying metal surface.

The Bader analysis of the charge density shows an appreciable charge transfer from the surface to the molecule which in this way attempts to achieve a closed shell electronic structure. Finally, an almost linear correlation is found between the calculated adsorption energy and the total charge in the adsorbate. This correlation confirms that the interaction between the ethoxy moiety and the transition metal surfaces studied in the present work is essentially electrostatic and originates from the response of the metallic surface to the charge on adsorbate.

The present conclusions are obtained from a few representative transition metal surfaces but in the view of the results it is likely that this will also be the case for other metallic surfaces as well.

Acknowledgments This work is dedicated to the memory of Jean Pierre Daudey, a great quantum chemist and a very generous person. J.R. (CVU 88721) thanks the Mexican CONACyT for a postdoctoral fellowship. Financial support has been provided by the Spanish MICINN (grants MAT2006-14274-C02-01 and FIS2008-02238) and Generalitat de Catalunya (grants 2009SGR1041 and XRQTC). Generous allocation of computational time from the Barcelona Supercomputing Center (BSC) is gratefully acknowledged.

References

1. Atkinson R (1997) J Phys Chem Ref Data 26:215–290
2. Atkinson R (1997) Int J Chem Kinet 29:99–111
3. Yamamoto Y, Asao N (1993) Chem Rev 93:2207–2293
4. Mendez M, Munoz MP, Nevado C, Cardenas DJ, Echavarren AM (2001) J Am Chem Soc 123:10511–10520
5. Dess DB, Martin JC (1991) J Am Chem Soc 113:7277–7287
6. Mallat T, Baiker A (2004) Chem Rev 104:3037–3058
7. March J (1993) Advanced organic chemistry: reactions mechanisms and structures, 3rd edn. McGraw-Hill, New York
8. Sheldon RA (1995) In: Sheldon RA, van Santen RA (eds) Catalytic oxidation. World Scientific Publishing, Singapore
9. Sheldon RA, Kochi JK (1981) Metal-catalyzed oxidations of organic compounds. Academic Press, New York
10. Yamaguchi K, Mizuno N (2002) Angew Chem Int Ed 41:4538–4541
11. Yamaguchi K, Mizuno N (2003) Chem Eur J 9:4353–4361
12. Mori K, Hara T, Mizugaki T, Ebitani K, Kaneda K (2004) J Am Chem Soc 126:10657–10666
13. Grunwaldt JD, Caravati M, Baiker A (2006) J Phys Chem B 110:25586–25589
14. Ferri D, Mondelli C, Krumeich F, Baiker A (2006) J Phys Chem B 110:22982–22986
15. Zhang ZX, Chen P, Liu J, Zhang YH, Shen W, Xu HL, Tang Y (2008) Chem Commun 3290–3292
16. Shimizu K, Sugino K, Sawabe K, Satsuma A (2009) Chem Eur J 15:2341–2351
17. Carrettin S, McMorn P, Johnston P, Griffin K, Hutchings GJ (2002) Chem Commun 696–697
18. Abad A, Concepción P, Corma A, García H (2005) Angew Chem Int Ed 44:4066–4069
19. Abad A, Corma A, García H (2008) Chem Eur J 14:212–222
20. Della Pina C, Falletta E, Rossi M (2008) J Catal 260:384–386
21. Guan Y, Hensen EJM (2009) Appl Catal A 361:49–56
22. Zaccheria F, Ravasio N, Psaro R, Fusi A (2006) Chem Eur J 12:6426–6431
23. Huang L, Zhu Y, Huo C, Zheng H, Feng G, Zhang C, Li Y (2008) J Mol Catal A 288:109–115
24. Comotti M, Della Pina C, Matarrese R, Rossi M (2004) Angew Chem Int Ed 43:5812–5815
25. Clotet A, Valcarcel A, Ricart JM, Illas F (2004) J Phys Chem B 108:18297–18305
26. Valcarcel A, Clotet A, Illas F, Ricart JM (2007) Phys Chem Chem Phys 9:311–317
27. Andersson MP, Uvdal P (2004) Surf Sci 549:87–96
28. Crapper MD, Woodruff DP, Bader M, Haase J (1987) Surf Sci 182:L241–L247
29. Camplin JP, McCash EM (1996) Surf Sci 360:229–241
30. Street SC, Gellman AJ (1996) J Chem Phys 105:7158–7170
31. Street SC, Gellman AJ (1996) J Phys Chem 100:8338–8348
32. Skoplyak O, Barteau MA, Chen JG (2008) Surf Sci 602:3578–3587
33. Gomes JRB, Gomes JANF, Illas F (1999) Surf Sci 443:165–176
34. Gomes JRB, Gomes JANF (2001) Surf Sci 471:59–70
35. Greeley J, Mavrikakis M (2002) J Catal 208:29–300
36. Li X, Gellman AJ, Sholl DS (2006) Surf Sci 600:L25–L28
37. Remediakis IN, Pedersen FA, Norskov JK (2004) J Phys Chem B 108:14535–14540
38. Chen ZX, Neyman KM, Lim KH, Rösch N (2004) Langmuir 20:8068–8077
39. Greeley J, Mavrikakis M (2002) J Am Chem Soc 124:7193–7201
40. Li X, Gellman AJ, Sholl DS (2005) J Mol Catal A 228:77–82
41. Perdew JP, Chevary JA, Vosko SH, Jackson KA, Pederson MR, Singh DJ, Fiolhais C (1992) Phys Rev B 46:6671–6687
42. Perdew JP, Chevary JA, Vosko SH, Jackson KA, Pederson MR, Singh DJ, Fiolhais C (1993) Phys Rev B 48:4978
43. Perdew JP, Wang Y (1992) Phys Rev B 45:13244–13249
44. Kresse G, Furthmüller J (1996) Comput Mat Sci 6:15–50
45. Kresse G, Furthmüller J (1996) Phys Rev B 54:11169–11186
46. Blöchl PE (1994) Phys Rev B 50:17953–17979
47. Kresse G, Joubert D (1999) Phys Rev B 59:1758–1775
48. Monkhorst HJ, Pack JD (1976) Phys Rev B 13:5188–5192
49. Kokalj A (1999) J Mol Graph Model 17:176–179
50. Schaftenaar G, Noordik JH (2000) J Comput-Aided Mol Design 14:123–134
51. Bader FW (1990) Atoms in molecules: a quantum theory. Oxford Science, Oxford, UK
52. Sanville E, Kenny SD, Smith R, Henkelman G (2007) J Comput Chem 28:899–908
53. Bagus PS, Hermann K, Bauschlicher CW (1984) J Chem Phys 80:4378–4386
54. Bagus PS, Illas F (1992) J Chem Phys 96:8962–8970
55. Cruz Hernandez N, Zicovich-Wilson CM, Sanz JF (2006) J Chem Phys 124:194105
56. Migani A, Illas F (2006) J Phys Chem B 110:11894–11906